Lab on a Chip

Detection and quantification of subtle changes in red blood cell density using a cell phone

Journal:	*Lab on a Chip*
Manuscript ID	LC-ART-03-2016-000415.R3
Article Type:	Paper
Date Submitted by the Author:	01-Jul-2016
Complete List of Authors:	Felton, Edward; Beth Israel Deaconess Medical Center, Medicine Velasquez, Anthony; Beth Israel Deaconess Medical Center, Medicine Lu, Shulin; Beth Israel Deaconess Medical Center, Medicine Murphy, Ryann; Beth Israel Deaconess Medical Center, Medicine ElKhal, Abdala; Beth Israel Deaconess Medical Center, Medicine Mazor, Ofer; Harvard Medical School Gorelik, Pavel; Harvard Medical School Sharda, Anish; Beth Israel Deaconess Medical Center, Medicine Ghiran, Ionita ; Beth Israel Deaconess Medical Center, Medicine

Detection and Quantification of Subtle Changes in Red Blood Cell Density Using a Cell Phone

Edward J. Felton[1], Anthony Velasquez[1], Shulin Lu[1], Ryann O. Murphy[1], Abdala ElKhal[1], Ofer Mazor[2], Pavel Gorelik[2], Anish Sharda[1], and Ionita C. Ghiran[1]

[1] Department of Medicine, Beth Israel Deaconess Medical Center and Harvard Medical School, Boston, MA 02115, USA

[2] Department of Neurobiology and Research Instrumentation Core Facility, Harvard Medical School, Boston, MA 02115, USA

Abstract

Magnetic levitation has emerged as a technique that offers the ability to differentiate between cells with different densities. We have developed a magnetic levitation system for this purpose that distinguishes not only different cell types but also density differences in cells of the same type. This small-scale system suspends cells in a paramagnetic medium in a capillary placed between two rare earth magnets, and cells levitate to an equilibrium position determined solely on their density. Uniform reference beads of known density are used in conjunction with the cells as a means to quantify their levitation positions. In one implementation images of the levitating cells are acquired with a microscope, but here we also introduce a cell phone-based device that integrates the magnets, capillary, and a lens into a compact and portable unit that acquires images with the phone's camera. To demonstrate the effectiveness of magnetic levitation in cell density analysis we carried out levitation experiments using red blood cells with artificially altered densities, and also levitated those from donors. We observed that we can distinguish red blood cells of an anemic donor from those that are healthy. Since a plethora of disease states are characterized by changes in cell density magnetic cell levitation promises to be an effective tool in identifying and analyzing pathologic states. Furthermore, the low cost, portability, and ease of use of the cell phone-based system may potentially lead to its deployment in low-resource environments.

1 Introduction

Cell density (the ratio of a cell's mass to its volume) has been shown to change during a variety of cell processes, and accordingly has the potential to offer insights into cell physiology and pathophysiology. Among the processes and behaviors associated with altered cell density are differentiation,[1,2] cell cycle progression,[3-6] apoptosis,[7-10] and malignant transformation.[11-14] Density, therefore, can be used as a criterion not only for differentiating between cells of different types, but also for distinguishing between cells of the same type, which enables experiments that target particular sub-populations identified by density and analysis in which density serves as in indicator of pathology.

Red blood cells (RBCs) are one cell type for which cell density analysis has played a significant role. The progressive increase of RBC density with age was established over 50 years ago,[15,16] and more recently the phenomenon of RBC terminal density reversal was discovered.[17] In sickle cell disease, density fractionation of RBCs was essential to revealing the heterogeneity of their age and hydration state, and helped elucidate the ion transport pathology responsible for RBC dehydration.[18] The increase in hemoglobin density caused by this phenomenon was shown to exacerbate RBC sickling and trigger hemolytic and vaso-occlusive episodes in this disease. In hereditary spherocytosis, differences in the structure of several membrane proteins were shown to be associated with altered RBC density.[19] The decrease of RBC density in the parasitic diseases malaria and babesiosis is well established, and forms the basis for techniques used to investigate and diagnose these disorders.[20-22] Additionally, iron deficiency anemia is characterized by a decrease in mean cell hemoglobin content of greater magnitude than the concomitant reduction in mean cell volume, resulting in a decrease in RBC density.[23]

Density gradient centrifugation has been used for decades as the standard technique for fractionating cells and subcellular components by density, and evaluation of RBCs by this method[15,16] led to the density-based phenomena highlighted above. This robust approach, however, requires the use of specialized gradient media as well as centrifuge equipment. Other techniques that have been developed for cell density analysis include acoustic microscopy of adherent cells,[24] and more recently ultrasound biomicroscopy,[25] optically induced electrokinetics,[26] acoustophoresis,[27,28] iso-acoustic focusing.[29] These methods offer wide versatility, but make use of customized apparatus that require expertise to fabricate and operate. Additionally, the suspended microchannel resonator[30,31] is capable of high-precision mass and density measurements, although its device is made via sophisticated microfabrication and relies on an advanced optical or electronic system for detection.

We previously introduced a method that employs magnetic levitation to differentiate cells based upon density, and demonstrated its ability to separate spatially both mixtures of different cell types and cells of the same type that have undergone physiological changes resulting in density differences.[32] This is accomplished by suspending cells in a paramagnetic gadolinium solution in a capillary, which is placed between two rare earth magnets with like poles facing each other. The cells respond to the magnetic, gravitational, and buoyant forces, and come to rest at an equilibrium position that depends on their densities. The apparatus was initially designed to work with a research-grade microscope that captures images of the levitating cells. In this work we present a novel compact and portable magnetic levitation device designed for use with a

smartphone. This device makes use of the same magnetic levitation device as the microscope-based system previously reported, but requires only ambient light for sample illumination and the smartphone's optical interface for image capture. In addition to the phone itself, it requires only inexpensive parts, including the rare earth magnets, an objective lens, and a plastic bracket that attaches to a smartphone case (Fig. 1C – 1G; Table 1). The use of smartphones as medical diagnostic devices has emerged as a new imaging and analysis platform with several groups reporting the their use for analysis of blood-borne parasites,[33] protein detection using ELISA,[34] and screening for HIV, tuberculosis, and malaria.[35]

We also introduce and characterize a new analysis method that determines the position of levitating cells relative to the levitation heights of reference beads with higher and lower densities, enabling comparisons among different samples in a quantified way. To our knowledge, previous magnetic levitation implementations do not determine the difference in cell density per micron of levitation height difference. With this method we demonstrate the sensitivity of the magnetic levitation technique using RBCs with densities modified by suspension in solutions of different tonicities, and establish an approximate range of detection for hemoglobin concentration achievable with the system. Additionally, we levitated blood samples from multiple donors, and in doing so identified one sample from an anemic donor.

Density analysis of blood cells with our platform needs only a drop of blood obtained via finger prick, a small quantity of gadolinium solution, and a disposable glass capillary. Levitated cells are ready for imaging within 15 minutes of loading the capillary. When incorporated with a smartphone, the portability, inexpensive components, and ease of use of this device offer the potential for implementation in low-resource environments as a tool for detection of blood diseases known to result in cell density changes.

2 Materials and Methods

2.1 Preparation of RBCs

The study was approved by the Beth Israel Deaconess Medical Center Institutional Review Board. 10 to 20 μL of fresh whole blood was obtained via venipuncture or finger prick from laboratory volunteers. Cells were washed twice and re-suspended in HBSS with calcium and magnesium (HBSS++) to a concentration of 5×10^3 cells/mL. Hemoglobin concentration values were obtained with a hemoglobinometer (Hb 201+, HemoCue, Ängelholm, Sweden).

2.2 Separation of new and old RBCs

Fresh whole blood (1 mL) obtained by venipuncture was washed twice, re-suspended in 1 mL of HBSS++, and loaded on top of 20 mL of self-forming Percoll gradient solution (30.76 mL Percoll (density 1.130 g/mL, GE Healthcare Bio-Sciences, Uppsala, Sweden), 4 mL 1.5 M NaCl, and 5.24 mL of deionized water) in a 30 mL tube. After centrifugation at 27,000 × g for 20 minutes multiple layers of RBCs of different densities were formed, with the least dense (newest) in the top layer and the most dense (oldest) in the bottom layer, as seen in Fig. 2C. RBCs from the top and bottom layers were extracted separately, washed twice, and re-suspended in HBSS++ at a concentration of 5×10^5 cells/mL.

2.3 Separation of Lymphocytes and Neutrophils

A syringe prefilled with 2.3 mL of 6% Dextran 500 (Sigma-Aldrich, St. Louis, MO) and 1 mL of 3.2% sodium citrate (Sigma-Aldrich) was used to draw fresh whole blood to a final volume of 10 mL. After gentle mixing the blood was sedimented for 45 minutes with the syringe's nozzle up. The RBC-free fraction was layered above 15 mL of Ficoll-Paque PREMIUM (density 1.077 g/mL, GE Healthcare Bio-Sciences) in a 50 mL tube and centrifuged at 500 × g for 10 minutes, after which lymphocytes were located at the plasma-Ficoll interface and neutrophils were pelleted at the bottom. The lymphocytes were collected and set aside, and the neutrophils were resuspended in 0.5 mL of HBSS++ and transferred to a new 50 mL tube. To lyse remaining RBCs 20 mL of 0.2% NaCl was added for 45 seconds, followed by 20 mL of 1.6% NaCl. The tube was then centrifuged at 500 × g for 10 minutes, and the resulting pellet was re-suspended in 0.5 mL of HBSS++. After isolation, lymphocytes and neutrophils were washed twice and re-suspended in HBSS++ at a concentration of 5×10^5 cells/mL.

2.4 Magnetic Levitation of Cells

Cells (final 5×10^3 cells/mL) suspended in HBSS++ were mixed with gadobenate dimeglumine solution (MutiHance, Bracco Diagnostics, Monroe Township, NJ), a strongly paramagnetic gadolinium (Gd^{3+})-based contrast medium. Mixtures of new and old RBCs were levitated in a solution with a final Gd^{3+} concentration of 30 mM, and 40 mM Gd^{3+} was used for RBC, neutrophil, and lymphocyte mixtures. Experiments that quantified RBC levitation height were done with a Gd^{3+} concentration of 50 mM or 60 mM, and two types of polymer microspheres were added to serve as reference particles of known density: 10 μm polystyrene beads (1.05 g/mL, Flow-Count Fluorospheres, Beckman Coulter, Brea, CA) and 9.9 μm PMMA beads (1.2 g/mL, Bangs Laboratories, Fishers, IN). These two beads were selected due to their highly uniform densities, whereas others we purchased were unsuitable for use as reference beads because they exhibited significant variation in levitation height. The 1.05 g/mL microspheres were diluted 1:100. A sonicated suspension stock of the 1.2 g/mL microspheres in HBSS++ was made at 5 mg/mL and used at 1:500 dilution.

Cell levitation was performed in square glass microcapillaries with a 1 mm × 1 mm cross section and 50 mm length (VitroCom, Mountain Lakes, NJ). To prevent cells from drifting during analysis Critoseal (Fisher Scientific, Pittsburgh, PA) was inserted into each end. We did not observe cell adhesion to the capillary walls. The magnetic field used for levitation was produced by positioning N52-grade NdFeB magnets with dimensions 1 mm × 5 mm × 50 mm (K&J Magnetics, Pipersville, PA) above and below the capillary with like poles facing each other, resulting in a 1 mm separation. The magnets were magnetized perpendicularly through the 1 mm x 50 mm surfaces, and had a surface field of 0.375 T. The magnitude and direction of the magnetic field produced by this configuration inside the capillary are shown in supplemental Fig. S1, both in a cross section of the capillary and along its length.

2.5 RBC Volume Measurement

RBCs were suspended in hypotonic (219 and 252 mOsmol/kg water), isotonic (287 mOsmol/kg

water), and hypertonic (371 and 455 mOsmol/kg water) mixtures of HBSS++, water, and Gd^{3+} (at a final concentration 50 mM). After equilibration for 15 minutes we measured the volume of each sample three times with a Coulter counter (Z2 Cell and Particle Counter, Beckman Coulter, Miami, FL). Similarly prepared RBC suspensions with reference beads were analyzed with magnetic levitation.

2.6 Microscopy

An Olympus AX70 Provis microscope was placed on its side to enable imaging through the side of the capillary (Fig. 1A and 1B) with a 10X, 0.40 numerical aperture (NA) objective. In this configuration, the magnetic, gravitational, and buoyant forces responsible for the cells' levitation are properly aligned. Micromanipulation stages (Thorlabs, Newton, NJ) were used to adjust the length and vertical position of the capillary with respect to the objective, and to focus on the cells within. The microscope stage was removed to allow for Kohler illumination, with the condenser positioned at the proper distance from the capillary glass. Images were acquired with a QImaging EX*i* CCD camera and IPLab software (BD Biosciences, Rockville, MD). For RBCs images were taken 15 minutes after inserting the capillary between the magnets, and for mixtures of new and old RBCs or RBCs with neutrophils and lymphocytes images were acquired after 25 minutes.

2.7 Cell Phone Imaging

A schematic of the device designed to enable imaging of levitating cells with an iPhone 5c is shown in Fig. 1C, along with an image of the device attached to the iPhone (Fig. 1D and 1E). The device incorporates an aspheric 6.33 mm diameter, 0.72 NA lens with anti-reflection coating (Edmund Optics, Barrington, NJ) flush against the iPhone's lens, and positions the capillary in line with the optical center of the lens and between the two magnets. Two adjustment knobs (Thorlabs) are used to focus the capillary (Fig. 1F). The device's components were designed with Adobe Illustrator (Adobe Systems, San Jose, CA), and fabricated from acrylic using a laser-cutting machine (PLS6.150D, Universal Laser Systems, Scottsdale, AZ). Parts were designed to friction fit onto a 0.060 inch-thick acrylic rectangle that was attached to an iPhone 5c case with adhesive (Fig. 1D).

To avoid any possible disruptive influences on the magnetic field within the capillary due to magnetic materials in the phone, the iPhone was inserted into its case once cells in the capillary reached their equilibrium position (15 minutes after loading cells). The standard iPhone Camera application was used to acquire images under the "noir" (black and white) setting (Fig. 1G). Full zoom was applied for maximum magnification, and the camera's "focus lock" feature was employed to maintain focus on the cells.

2.8 Image Analysis

Images taken with the microscope system were saved in .tiff format, and those acquired with the iPhone system were saved in .jpg format and converted to .tiff with IPLab. A background correction was also applied with IPLab to reduce variations in the background level. In subsequent analysis using Igor Pro software (Wavemetrics, Lake Oswego, OR) the average

intensity of each row of pixels was calculated and plotted against the row's position relative to the top of the image, as illustrated with the red trace in Fig. S2, resulting in peaks corresponding to the two beads and cells. Gaussian curves were fit to each peak (blue trace in Fig. S2) and the locations of the beads and cells were determined to be the peak locations of the fits. We then calculated the ratio of the distance between the cells and denser beads to the distance between the cells and less dense beads. This ratio, the *Levitaion Ratio,* was used to estimate and compare RBC densities in our experiments.

3 Results and Discussion

3.1 Image Quality and Density Resolution of Microscope and Cell Phone Levitation Systems

We investigated the relationship between levitation height and Gd^{3+} concentration, from 50 to 200 mM, and confirmed that it followed the expected behavior seen in Fig. S3A and derived in Supplementary Information Section S1. Concentrations below 50 mM did not provide enough magnetic force to lift the denser beads from the bottom of the capillary. Since levitation height is a linear function of density, we quantified the system's ability to resolve density spatially by calculating the ratio of the density difference of the reference beads to their levitation height difference. This ratio, the density resolution, measures the difference in density per micron of vertical separation for a given Gd^{3+} concentration, such that lower values correspond to higher resolutions (see Supplementary Information Section S2 for formula). The values for each concentration are plotted in Fig. S3B. The system's resolution is maximized at 50 mM with a value of 0.5×10^{-3} g/mL/μm, and decreases to 2.0×10^{-3} g/mL/μm at 200 mM.

We observed that after reaching their equilibrium positions cells remained there for the duration of the experiment, indicating that their densities and magnetic properties did not change and were not affected by the presence of the Gd^{3+}. Diffusion of Gd^{3+} into the cells is prevented by the size of the Gd^{3+} molecules, since they are chelated with large organic molecules, and the fact that they are hydrophilic. Additionally, Gd^{3+} cannot enter the cells via endocytosis or pinocytosis because RBCs lack these transport mechanisms.

Fig. 2 displays images of magnetically levitated cells acquired with both our microscope- and cell phone-based systems. The mixture of lymphocytes, neutrophils, and red blood cells in Fig. 2A separated into three distinct bands based on their density, as indicated by the three peaks in the intensity profiles to the right. Levitated RBCs, along with high- and low-density reference beads, are shown in Fig. 2B. A mixture of old and new RBCs obtained from a sample separated by density gradient centrifugation were levitated and shown to separate into the two distinct bands in Fig. 2C, demonstrating that the magnetic levitation systems have the ability to distinguish between cells of the same type with different densities.

Both of the systems produce high-resolution images in which individual levitating cells are resolved and the cells and reference beads are in focus. The lateral image resolution of each system is 1-2 μm, which is below the height of a RBC positioned in side view (2.2 μm). In order to achieve optimal magnetic levitation it is critical that the magnets be positioned without any tilt with respect to the gravitational field, as deviation from this condition results in a net force on

the cells towards the wall of the capillary. Proper orientation of the magnets also ensures that the equilibrium positions of levitating objects are all in a plane that is perpendicular to the objective (microscope) or lens (cell phone), allowing all of them to be in focus. For the microscope system the magnet and capillary assembly is mounted on three stackable translation stages (Fig. 1A and 1B); the objective's position is fixed and cells levitating in the capillary are brought into focus by moving the capillary into its object plane. For the cell phone system the capillary's position with respect to the camera's lens is controlled by adjustment knobs (Fig. 1F). The camera's lens is not fixed in position, and after initial adjustment of the focusing knobs is performed the camera moves its lens to bring the cells into final focus. Since the iPhone's lens is actuated by a voice coil motor, which contains a magnet, we wait until cells have reached their final levitation positions before inserting the phone into its case. We did not study whether the lens' magnet is strong enough to alter the magnetic field in the capillary, but we follow this procedure as a precautionary measure to avoid any potential interference.

The resolution of an optical system is dependent upon its NA. For the microscope-based system, resolution is aided by its high-quality optical components including a plan apochromatic objective with a NA of 0.40 and a condenser lens that provides Kohler illumination to the sample and doubles the system's NA. It also benefits from a scientific-grade CCD camera with its sensor located the optimal distance from the tube lens. The cell phone system lacks the aperture diaphragm and condenser lens necessary for optimal image contrast and proper illumination, and the condenser's contribution to overall NA is lost. To mitigate this it makes use of an aspheric lens with a numerical aperture of 0.72 that, in combination with the camera's lens, results in a system NA similar to that of the microscope system. This enables the cell phone imaging system to achieve image resolution comparable to that of the microscope, as shown in Fig. 2, despite the fact that the two systems have optical components, lights paths, and imaging sensors of different types, quality, and performance.

3.2 Analysis of RBCs with Different Densities

To evaluate the ability of magnetic levitation to measure differences in cell density we altered the volumes, and thus the densities, of RBCs by suspending them in buffers with different tonicities. Suspension in hypertonic buffer causes cell dehydration, resulting in smaller volume and higher cell density, while suspension in hypotonic buffer leads to "overhydrated" cells with increased volume and reduced density. We chose a range of tonicities for which the most hypertonic solution (456 mOsmol/kg water) produced several cells per image with changed morphology (from round to crenate), and the most hypotonic solution (219 mOsmol/kg water) yielded only a few cells per image that ruptured due to increased osmotic pressure. RBCs from one donor sample were suspended in the different buffers and levitated, and images of these are displayed in Fig. 3A. We analyzed the images to determine the levitation ratio of each sample, and plotted the ratio as a function of tonicity in Fig. 3B. The observed decrease in RBC levitation ratio with increasing buffer tonicity reflects the anticipated decrease in density. We noted that the widths of the cell bands in Fig. 3A were unchanged for all but the 456 mOsmol/kg water sample, which had an increased width. We attribute this to the fact that this sample's solution was the most hypertonic sample used, and the erythrocyte fragility of the older cells in the population may have caused them to be more susceptible to osmotic pressure. This may also

be sample dependent, as not all RBC samples tested exhibited a cell band width different from that of cells in other tonicities.

We also measured the volumes of the RBCs with a Coulter counter in triplicate, and found that cells in buffers with tonicities had mean corpuscular volumes (MCVs) ranging from 64.2 ± 0.5 to 104.8 ± 3.5. RBCs in the isotonic buffer had a MCV of 89.5 ± 1.7 fL, which is within the accepted normal range of 80-100 fL.[36] A plot of the relationship between the levitation ratio and the measured MCVs is shown in Fig. 3C, indicating that RBCs with the same hemoglobin content levitate at higher positions as their volume increases and renders them less dense. In addition, to verify explicitly that the MCV changes were caused by immersion in buffers of increased tonicity we plotted relative volume versus the inverse of relative tonicity, where the relative volume (or tonicity) is the MCV (or tonicity) divided by the MCV (or tonicity) under isotonic conditions. This should be a linear relationship for volume changes caused by osmotic pressure, and our result (Fig. 3D) confirmed this to be true.

While these artificial density changes were the result of volume changes, density changes in disease state RBCs can be the result of changes to both cell volume and hemoglobin content. For example, anemia caused by decreased hemoglobin production, such as iron deficiency anemia and thalassemia, are characterized by decreased MCH and cell density.[23] Conversely, conditions associated with RBC dehydration, such as hereditary spherocytosis and hemoglobin C disease, are conditions in which MCH is elevated, lead to a density increase. Additionally, sickle cell disease is marked by a decrease in volume and MCH and a density increase. Regardless of the cause of density change, the magnetic levitation system offers the capability to distinguish between RBCs within the range of densities spanned by healthy and diseased cells.

3.3 Detection of Low Density RBCs in Iron Deficiency

RBCs were acquired from eleven self-reported healthy donors for analysis with magnetic levitation, and their hemoglobin concentrations were measured with a hemoglobinometer. Ten of the samples had hemoglobin concentrations between 12.3 and 15.9 g/dL. Images of these along with their levitation ratios are shown in Fig. 4A, and levitation ratio vs. hemoglobin concentration is plotted in Fig. 4B. Despite hemoglobin concentration variability between 12 and 16 g/dL the levitation ratios were clustered at around an average value of 3.47 ± 0.19, and samples with almost identical ratios had hemoglobin concentrations differing by as much as 3 g/dL. This apparent discrepancy is explained by the fact that in this range differences in hemoglobin concentration are primarily due to differences in the number of RBCs per volume of blood, rather than significant differences in the amount of hemoglobin per cell. This is also the predominant reason that males have higher hemoglobin concentrations than females; RBCs of both genders have the same MCV and MCH but the number of RBCs per volume of blood is higher for males.[37,38]

One of the eleven donor samples levitated at a noticeably higher rate than the others (levitation ratio of 5.27), as can be seen in the comparison in Fig. 4D between RBCs from one of the other ten donors (left) and this sample (right). The overlay of intensity profiles shows an upward shift indicating that this sample's RBCs are less dense. It had a hemoglobin concentration of 8.6 g/dL, much lower than the other ten, and in fact this donor was ultimately diagnosed with iron

deficiency anemia. Its ratio and hemoglobin concentration are also plotted in Fig. 4B. We evaluated the relative size of the anemic RBCs and those with hemoglobin concentration in the normal range by flow cytometry, and noted a reduction in size of the anemic cells in the overlay of forward scatter histograms in Fig. 4C. This volume reduction is commonly associated with iron deficiency anemia and is the result of the cells' diminished hemoglobin content.

To further explore the shift in levitation height we separated the RBCs levitated in Fig. 4D by density gradient centrifugation. In Fig. 4E there is an easily discernable band of low-density RBCs at the top of the anemic tube (right) that is above the lowest density band in the normal hemoglobin concentration tube (left). We extracted cells from the lowest density bands from each sample for magnetic levitation, as displayed in Fig. 4F, and observed a greater degree of levitation height difference between the two. The upward shift in levitation found when including all cells in each sample (Fig. 4D) resulted in an overlap of populations, such that least dense normal hemoglobin concentration RBCs and most dense anemic RBCs have equivalent densities, but comparison of just the lowest density cells of each sample results in an overlap-free shift. This is most likely because the newest RBCs experience the greatest density decrease from the untreated iron deficiency, whereas those that have been in circulation for some time have undergone subsequent age-related volume decrease.

Magnetic levitation of RBC samples from the eleven donors was performed with the microscope-based system, but we also conducted the comparison of the anemic and normal hemoglobin concentration RBCs with the cell phone-based system to confirm its ability to detect the lower density anemic RBCs. The cell phone images shown in Fig. 5 show the same difference in levitation height as those in Fig. 4D. In these images both cells and beads are adequately resolved, and the positions of the levitated RBCs produced the same intensity profile (at right) as the microscope-based system. Since both systems use the same magnetic apparatus obtaining the same result with the cell phone device is unsurprising.

4 Conclusions

We have developed a magnetic levitation-based method for analysis of cells by density, and demonstrated that it can be used to distinguish between cells, either of different types or of the same type that have undergone changes causing subtle density differences. As part of the method we introduced the use of reference beads that assist in quantifying the levitation height of cells to make possible comparisons between cells. We established its sensitivity in this work with RBCs, including those of a donor with anemia, but it is broadly applicable. For example, a subpopulation of low-density neutrophils have been discovered in patients with autoimmune disorders, sepsis, HIV infections, and cancer,[32] and could therefore be differentiated from healthy neutrophils by magnetic levitation. In addition, a more elaborate apparatus using microfluidics to deliver cells suspension into and out of the capillary offers the potential ability to collect the separated populations of a levitated cell mixture for further experimental use.

The integration of the magnetic levitation system with a smartphone for image acquisition has also been introduced here, and we have shown that the optical components of the smartphone-based magnetic levitation device produce images comparable to those of a microscope. Due to its small size, portability, and low cost of components and required reagents, the system could

serve as a powerful diagnostic tool in locations lacking sophisticated medical equipment. Furthermore, analysis requires only a drop of blood from a finger prick and produces a result in minutes at the point of care, without the need to transport it elsewhere. Access to local and inexpensive diagnostic care is critical for widespread diseases that affect millions such as malaria and anemia, and as smartphones become ubiquitous worldwide we anticipate that our device could have a significant impact in low-resource environments.

Acknowledgements

This work was supported by grants awarded to IG from the NIH (R01-HL096795 and R21-TW009915) and the Bill and Melinda Gates Foundation (OPP1032683).

References

1. D. Maric, I. Maric, W. Ma, F. Lahojuji, R. Somogyi, X. Wen, W. Sieghart, J. M. Fritschy, J. L. Barker, *Eur J Neurosci*, 1997, **9**, 507-522.

2. D. Maric, I. Maric, J. L. Barker, *Methods*, 1998, **16**, 247-259.

3. D. A. Wolff, H. Pertoft, *J Cell Biol*, 1972, **55**, 579-585.

4. K. Bienz, D. Egger, D. A. Wolff, *J Virol*, 1973, **11**, 565-574.

5. R. K. Poole, *J Gen Microbiol*, 1977, **98**, 177-186.

6. W. W. Baldwin, H. E. Kubitschek, *J Bacteriol*, 1984, **158**, 701-704.

7. V. E. Yurinskaya, A. V. Moshkov, Y. M. Rozanov, A. V. Shirokova, I. O. Vassilieva, E. V. Shumilina, F. Lang, E. V. Volgareva, A. A. Vereninov, *Cell Physiol Biochem*, 2005, **16**, 15-22.

8. A. H. Wyllie, R. G. Morris, *Am J Pathol*, 1982, **109**, 78-87.

9. R. G. Morris, A. D. Hargreaves, E. Duvall, A. H. Wyllie, *Am J Pathol*, 1984, **115**, 426-436.

10. R. S. Benson, S. Heer, C. Dive, A. J. Watson, *Am J Physiol*, 1996, **270**, 1190-1203.

11. A. Zipursky, E. Bow, R. S. Seshadri, E. J. Brown, *Blood*, 1976, **48**, 361-371.

12. C. Huber, K. Zier, G. Michlmayr, H. Rodt, K. Nilsson, H. Theml, D. Lutz, H. Braunsteiner, *Br J Haematol*, 1978, **40**, 93-103.

13. C. Huber, D. Lutz, D. Niederwiesser, G. Weiser, O. Dietze, H. Theml, H. Braunsteiner, *Blood*, 1982, **60**, 1397-1401.

14. C. Griwatz, B. Brandt, G. Assmann, K. S. Zänker, *J Immunol Methods*, 1995, **183**, 251-265.

15. E. R. Borun, W. G. Figueroa, S. M. Perry, *J Clin Invest*, 1957, **36**, 676-679.

16. R. C. Leif, J. Vinograd, *Proc Natl Acad Sci*, 1964, **51**, 520-528.

17. R. M. Bookchin, Z. Etzion, M. Sorette, N. Mohandas, J. N. Skepper, V. L. Lew, *Proc Natl Acad Sci*, 2000, **97**, 8045-8050.

18. V. L. Lew, R. M. Bookchin, *Physiol Rev*, 2005, **85**, 179-200.

19. M. Caterino, M. Ruoppolo, S. Orrù, M. Savoia, S. Perrotta, L. Del Vecchio, F. Salvatore, G. W. Stewart, A. Iolascon, *FEBS Lett*, 2006, **580**, 6527-6532.

20. G. B. Nash, E. O'Brien, E. C. Gordon-Smith, J. A. Dormandy, *Blood*, 1989, **74**, 855-861.

21. J. E. Mrema, G. H. Campbell, R. Miranda, A. L. Jaramillo, K. H. Rieckmann, *Bull World Health Organ*, 1979, **57**, 133-138.

22. A. Alkhalil, D. A. Hill, S. A. Desai, *Cell Microbiol*, 2007, **9**, 851-860.

23. J. M. England, S. M. Ward, M. C. Down, *Br J Haematol*, 1976, **34**, 589-597.

24. J. A. Hildebrand, D. Rugar, R. N. Johnston, C. F. Quate, *Proc Natl Acad Sci*, 1981, **78**, 1656-1660.

25. B. E. Treeby, E. Z. Zhang, A. S. Thomas, B. T. Cox, *Ultrasound Med Biol*, 2011, **37**, 289-300.

26. Y. Zhao, H. S. S. Lai, G. Zhang, G. B. Lee, W. J. Li, *Biomicrofluidics*, 2015, **9**, 022406.

27. F. Petersson, L. Åberg, A. M. Swärd-Nilsson, T. Laurell, *Anal Chem*, 2007, **79**, 5117-5123.

28. X. Ding, Z. Peng, S. C. S. Lin, M. Geri, S. Li, P. Li, Y. Chen, M. Dao, S. Suresh, T. J. Huang, *Proc Natl Acad Sci*, 2014, **111**, 12992-12997.

29. P. Augustsson, J. T. Karlsen, H. W. Su, H. Bruus, J. Voldman, Nat Commun, 2016, DOI: 10.1038/ncomms11556.

30. M. Godin, A. K. Bryan, T. P. Burg, K. Babcock, S. R. Manalis, *Appl Phys Lett*, 2007, **91**, 123121.

31. W. H. Grover, A. K. Bryan, M. Diez-Silva, S. Suresh, J. M. Higgins, S. R. Manalis, *Proc Natl Acad Sci*, 2011, **108**, 10992-10996.

32. S. Tasoglu, J. A. Khoory, H. C. Tekin, C. Thomas, A. E. Karnoub, I. C. Ghiran, U. Demirci, *Adv Mater*, 2015, **27**, 3901-3908.

33. M. V. D'Ambrosio, M. Bakalar, S. Bennuru, C. Reber, A. Skandarajah, L. Nilsson, N. Switz, J. Kamgno, S. Pion, M. Boussinesq, T. B. Nutman, D. Fletcher, *Sci Transl Med*, 2015, **7**, 286re4.

34. T. Laksanasopin, T. W. Guo, S. Nayak, A. A. Sridhara, S. Xie, O. O. Olowookere, P. Cadinu, F. Meng, N. H. Chee, J. Kim, C. D. Chin, E. Munyazesa, P. Mugwaneza, A. J. Rai, V. Mugisha, A. R. Castro, D. Steinmiller, V. Linder, J. E. Justman, S. Nsanzimana, S. K. Sia, *Sci Transl Med*, 2015, **7**, 273re1.

35. O. Mudanyali, S. Dimitrov, U. Sikora, S. Padmanabhan, I. Navruz, A. Ozcan, *Lab Chip*, 2012, **12**, 2678-2686.

36. K. Kaushansky, M. A. Lichtman, E. Beutler, T. J. Kipps, U. Seligsohn, J. T. Prchal, *Williams Hematology*, McGraw-Hill, New York, 2010.

37. W. G. Murphy, *Blood Rev*, 2014, **28**, 41-47.

38. P. Scapini, M. A. Cassatella, *Blood*, 2014, **124**, 710-719.

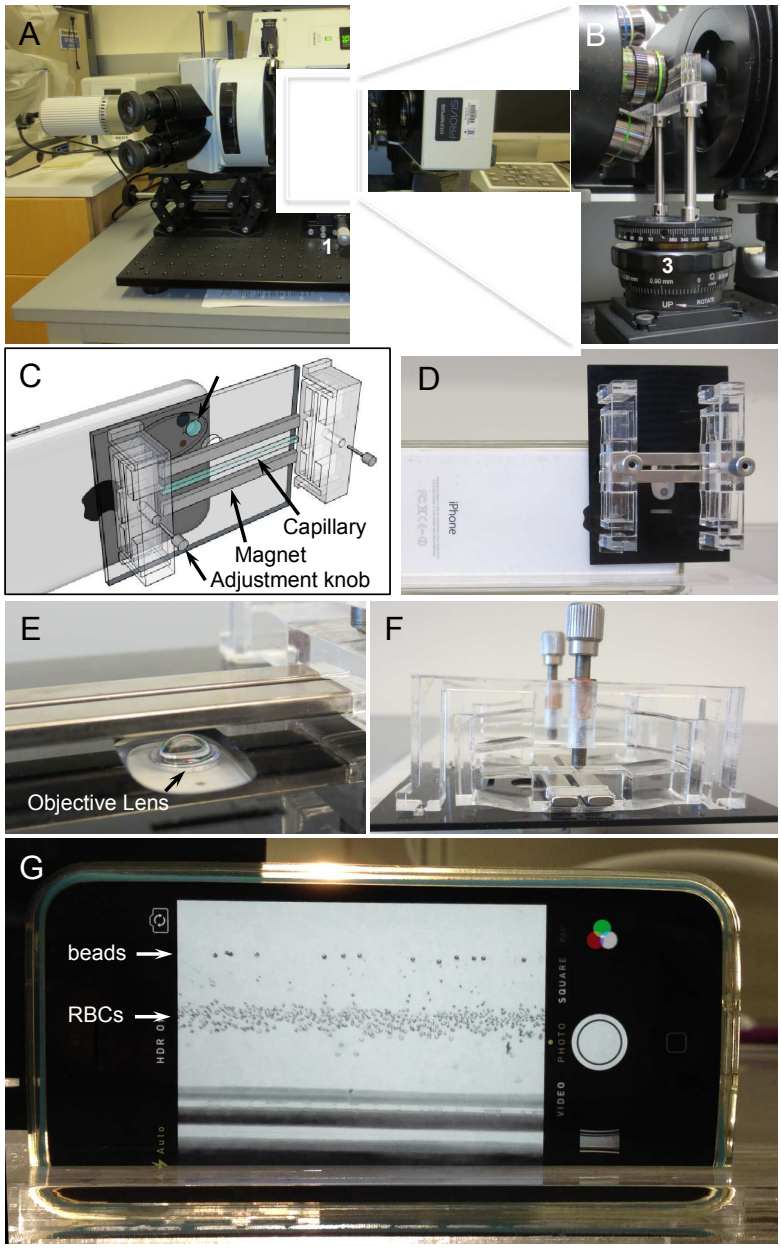

Fig. 1 Microscope and cell phone-based magnetic levitation platforms. (A) An Olympus Provis microscope placed on its side to enable imaging through the side of the capillary. Micromanipulators 1 and 2 adjust the position along the capillary's length relative to the objective and focus the cells, respectively. (B) Close-up image of the magnets and capillary relative to the objective. Micromanipulator 3 adjusts the capillary's height. (C) Schematic diagram of the magnets, capillary, and lens attached to the iPhone. (D) Image of the iPhone with attached magnetic levitation device. (E) Close-up view of the external aspheric lens positioned in line with the iPhone's lens. (F) Close-up image indicating the ability of the knobs to adjust the capillary's position with respect to the lens. (G) The iPhone's Photos application displaying levitated red blood cells and reference beads in the capillary.

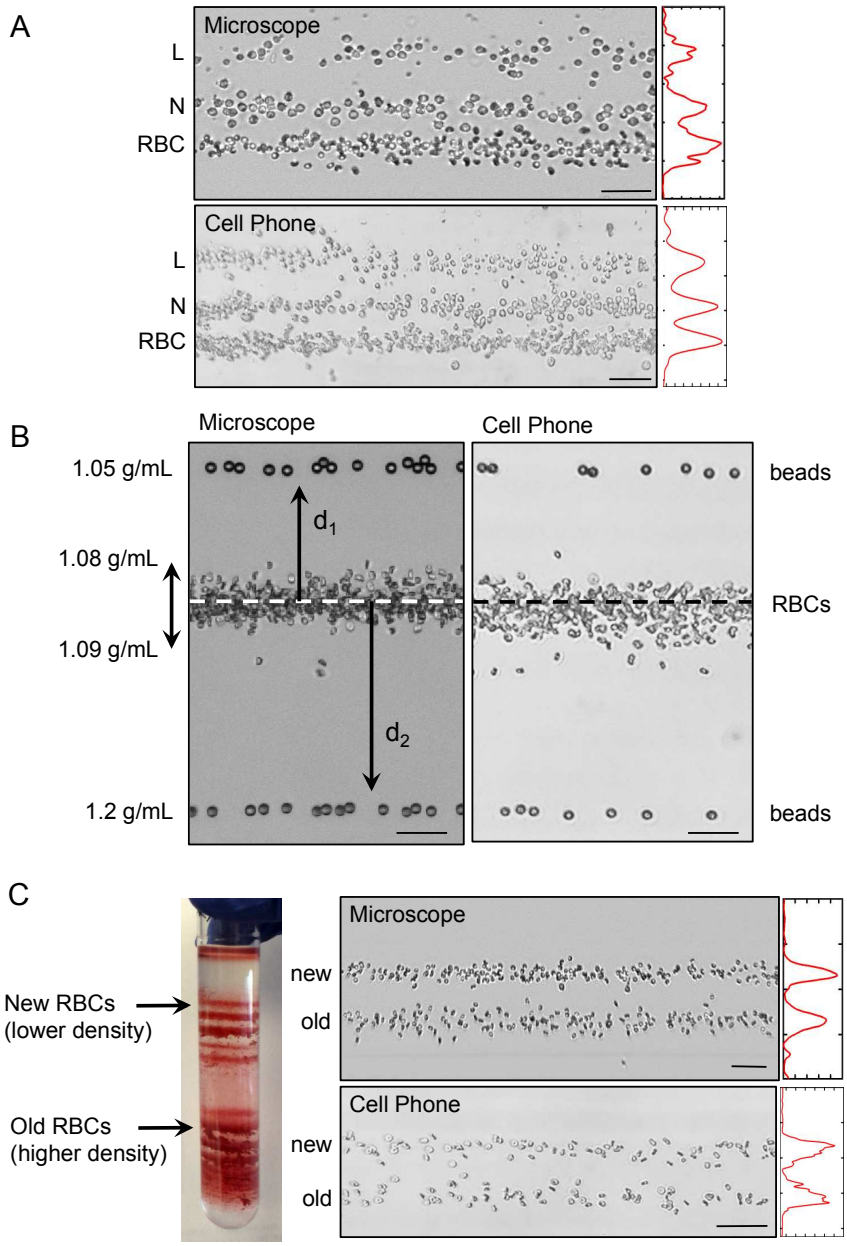

Fig. 2 Comparison of levitating cells with microscope- and cell phone-based systems. (A) Mixtures of lymphocyte, neutrophil, and red blood cells separated into bands with each system. Intensity profiles at right indicate positions of bands for lymphocytes (top), neutrophils (middle), and RBCs (bottom), denoted by L, N, and RBC, respectively. (B) Levitating RBCs imaged with each system, along with reference beads of lower and higher densities. Distances from the center of the cell bands to the reference beads, denoted as d_1 and d_2, are used to determine the levitation ratio. (C) RBCs of different ages separated via centrifugation in Percoll gradient solution. Extracted and mixed old and new RBCs levitated in two bands based on density. Band positions are indicated by the intensity profiles at right. All scale bars represent 50 μm.

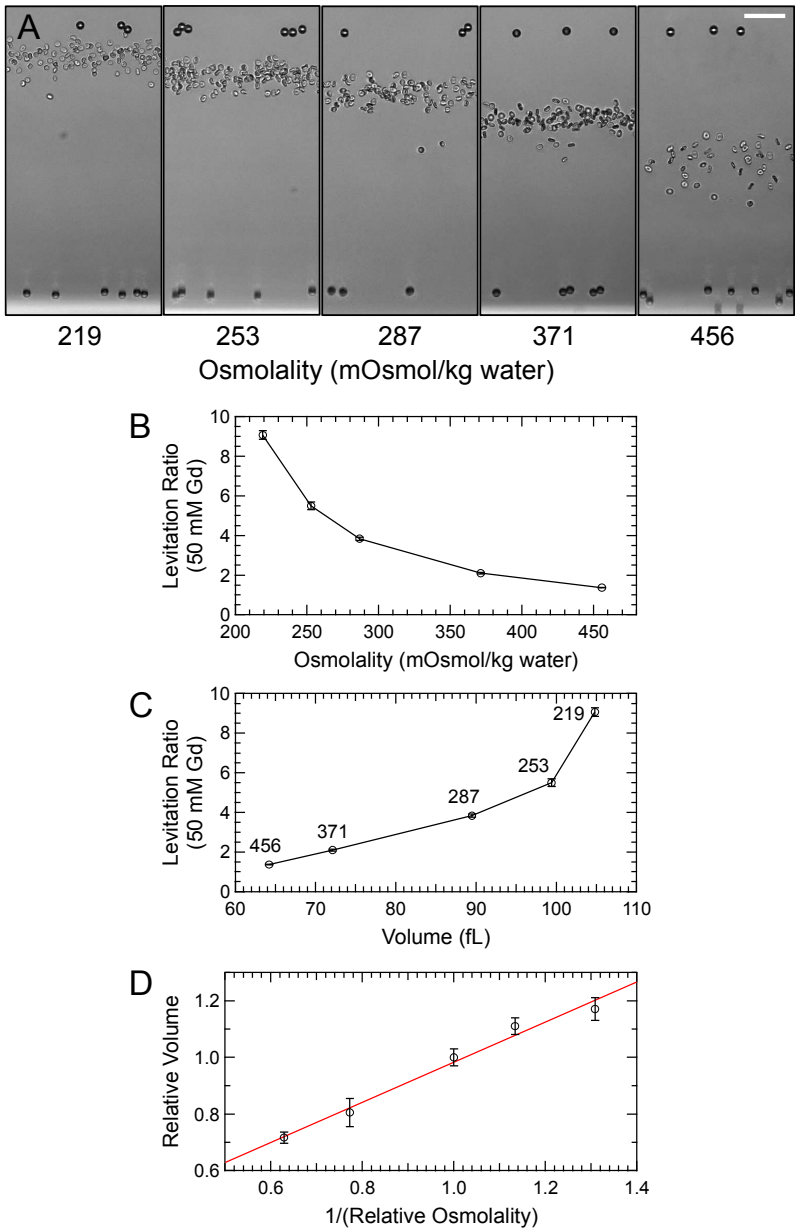

Fig. 3 Levitating RBCs with altered densities obtained by suspending cells in buffers with different osmolalities. (A) 10X microscope images of RBCs from the same sample levitated in hypertonic, isotonic, and hypotonic 50 mM Gd solutions, ranging from 219 to 456 mOsmol/kg water. Scale bar represents 50 µm. (B) Levitation ratio of RBCs from (A) plotted as a function of buffer osmolality. (C) Levitation ratio of RBCs as a function of average volume, as measured with a Coulter Counter. Numbers by each data point indicate buffer osmolality. Error bars in (B) and (C) are the standard deviations of the levitation ratios (N=5 for each). (D) Relative volume of RBCs plotted versus the inverse of relative osmolality, indicating the linear relationship characteristic of osmotic changes to cell volume (linear regression r-squared value 0.99). Error bars are the standard deviations of the volume measurements (N=3 for each).

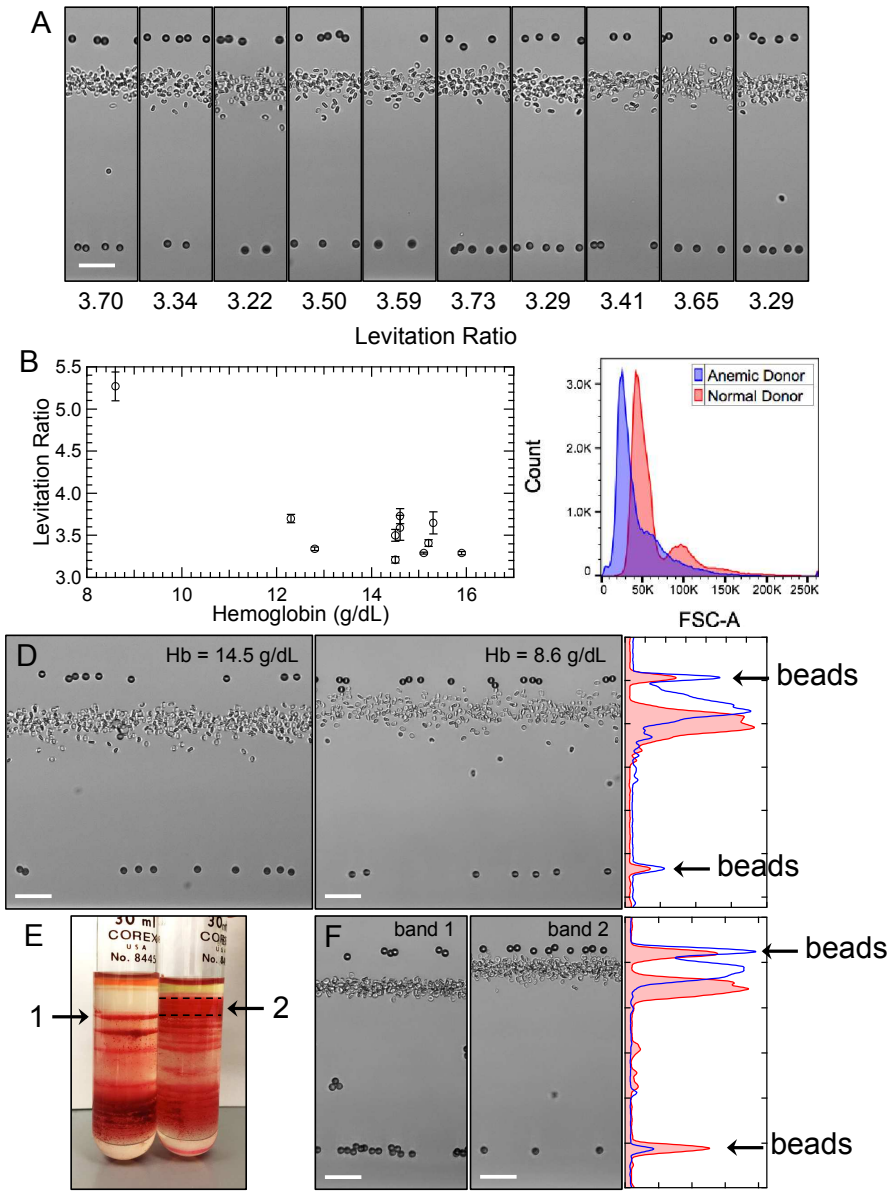

Fig. 4 Levitation and hemoglobin concentrations of RBCs from donors. (A) Microscope images of donor RBC samples levitated in isotonic 60 mM Gd solution, with corresponding levitation ratios between 3 and 4 (N=3 for each). (B) Levitation ratio vs. hemoglobin concentration for all donors, including the anemic outlier with hemoglobin 8.6 g/dL and levitation ratio of 5.3 ± 0.2 (N=3). (C) Overlay of flow cytometry forward scatter histograms of RBCs from donors with normal (red) and anemic (blue) hemoglobin concentrations, illustrating the smaller average size of RBCs from the anemic donor. (D) Microscope images of a donor sample from the normal range compared to the anemic donor, along with intensity profiles of the normal (red) and anemic (blue) donors. (E) Percoll density gradient of the samples imaged in (D), with a clearly distinguished band of less dense cells in the anemic donor sample (right tube). The top bands for the normal and anemic donor are labeled 1 and 2, respectively. (F) Microscope images of levitated cells extracted from bands 1 and 2, along with intensity profiles for band 1 (red) and band 2 (blue). All images acquired at 10X and all scale bars represent 50 μm.

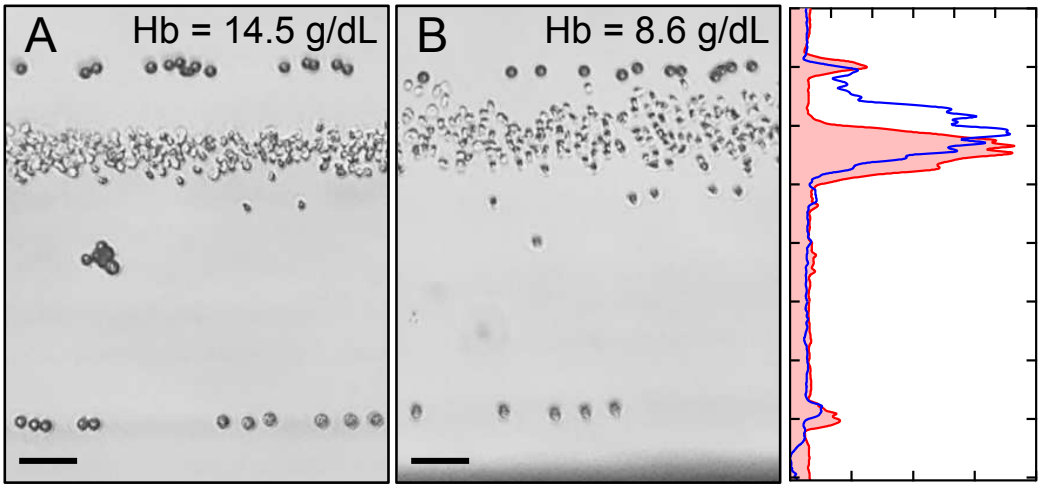

Fig. 5 Magnetically levitated RBCs with reference beads imaged with the iPhone device and Photos app. RBCs from (A) a donor with normal hemoglobin contrasted with (B) the anemic donor. Intensity profiles of the normal (red) and anemic (blue) hemoglobin donor cells are shown to the right. Scale bars represent 50 μm.

Table 1. Cost of iPhone Device Parts

Item	Cost (USD)
Objective Lens	25.00
iPhone 5c Case	7.50
Acrylic Bracket	6.25
Acrylic Rectangle	1.00
Adjustment Thumb Screws (2)	0.75
Rare Earth Magnets (2)	0.75
Capillary (disposable)	1.00
Critoseal*	3.50

*Enough for several hundred capillaries.